Studying Molecular 3D Structure and Dynamics by High-Resolution Solid-State NMR: Application to l-Tyrosine-Ethylester

Karsten Seidel,[†] Manuel Etzkorn,[†] Lars Sonnenberg,[†] Christian Griesinger,[†] Angelika Sebald,*[,‡] and Marc Baldus*[,†]

Max-Planck-Institute for Biophysical Chemistry, Department of NMR-Based Structural Biology, Am Fassberg 11, 37077 Göttingen, Germany, and Bayerisches Geoinstitut, University of Bayreuth, 95440 Bayreuth, Germany

Received: September 28, 2004; In Final Form: January 17, 2005

A unified approach to the study of 3D conformation and molecular dynamics using magic-angle-spinning solid-state NMR is demonstrated on a uniformly ^{13}C-labeled sample of l-tyrosine-ethylester.

1. Introduction

Solid-state nuclear magnetic resonance (NMR) has recently made considerable progress in studying molecular structure in systems that are insoluble or do not exhibit long-range structural order.[1−3] In addition to advancements regarding instrumentation and access to ultrahigh magnetic fields, NMR concepts have been proposed to probe three-dimensional molecular structure in high spectral resolution. These techniques include the combined measurements of individual internuclear distances and molecular torsion angles,[2,4] a structural analysis based on the use of several multiply labeled samples,[3,5] and the determination of 3D molecular structure from a single (uniformly isotope-labeled) sample.[6,7]

In addition to the study of molecular structure, solid-state NMR also provides unique means to probe molecular dynamics on a wide time scale.[8] For more than two decades, powerful applications have been reported, ranging from probing chain order in lipids[9] and polymers[10] to the investigation of backbone and side-chain motion in (membrane) proteins.[11] Many applications have relied on studying anisotropic NMR interactions to monitor dynamics or have invoked relaxation measurements that are capable of probing molecular dynamics without interference effects from the overall (isotropic) tumbling of the molecule in the solution state. Such studies, for example, can deliver order parameters to describe segmental motion in terms of amplitude fluctuations and may be used to study aromatic ring flips, side-chain motion in polypeptides, methyl group rotations, or structural phase transitions.

As has been known for a long time (see, for example, ref 12 and references therein) and recently shown for the case of l-tyrosine-ethylester (TEE),[13] dynamic disorder affects many solid materials, including those made from small molecules. Molecular crystalline solids such as TEE thus are ideal test systems to establish general concepts for monitoring 3D structure and dynamics using a single (uniformly) labeled sample. In the following, we demonstrate that solid-state NMR methods tailored to 3D structure determination of uniformly labeled biomolecules under magic-angle spinning (MAS)[14] conditions in conjunction with techniques that probe local motion in a site-resolved manner can provide complementary insight into the details of molecular structure and dynamics in solid-phase systems. Such studies not only may aid the structural characterization of (bio)polymers and (membrane) proteins but also may be used to study the relationship between free and receptor-bound conformations of a variety of pharmacophores of small molecular weight.[15]

2. Material and Methods

2.1. Sample Preparation. All solid-state NMR experiments discussed in the following were conducted on a diluted, uniformly ^{13}C-labeled sample of l-tyrosine-ethylester (TEE) (see also refs 13,16) (Figure 1). 3D structural information was obtained using an NMR sample diluted at 10% in unlabeled TEE (*U*-[^{13}C]TEE$_{dil}$). For this purpose, 4.5 mg of *U*-[^{13}C]TEE and 45 mg of TEE with ^{13}C in natural abundance were dissolved in ethanol. After overnight evaporation of the solvent, the sample was ground and dried in a vacuum desiccator prior to transferring it into a standard 4-mm MAS rotor.

2.2. NMR Experiments. Two-dimensional (^{13}C,^{13}C) CHHC and CHC correlation experiments were carried out on a Bruker Avance 600 (Bruker Biospin, Germany) spectrometer at 14.1 T equipped with a standard 4-mm Bruker MAS probe, at a spinning speed of 9.5 kHz. Rotational resonance in the tilted rotating frame (R^2TR) and Lee−Goldburg cross polarization (LG-CP) buildup experiments were performed on an Avance 400 spectrometer at 9.4 T using a 4-mm rotor, at spinning speeds described below. For evolution and detection periods, TPPM[17] proton decoupling was used.

Two-dimensional CHHC correlation spectroscopy was done according to methods described earlier[7,18,19] using longitudinal (0Q) ^{1}H−^{1}H mixing in the laboratory frame. CH transfer steps bracketing the (^{1}H ↔ ^{1}H) mixing unit were set to 125 μs. CHHC experiments were conducted on *U*-[^{13}C]TEE$_{dil}$ at 261 K for 75, 150, 250, and 500 μs ^{1}H−^{1}H mixing times, with 312 points sampled in the indirect dimension, and 288, 128, 128, and 256 transients acquired per evolution period, respectively. At higher temperature (318 K), three 2D CHHC spectra with a ^{1}H−^{1}H mixing time of 250 μs and CHHC cross polarization (CP) contact times of 175 μs were recorded over a time of 3.5 days and added together.

In Figure 2, the pulse scheme for a 2D CHC correlation experiment is shown. After an initial CP (cross polarization[20]) transfer and a *z*-filter to remove any residual ^{1}H magnetization,

* Corresponding authors. Telephone/fax: +49-551201-2212/2202. E-mail: angelika.sebald@uni-bayreuth.de, or maba@mpibpc.mpg.de.
[†] Max-Planck-Institute for Biophysical Chemistry.
[‡] Bayerisches Geoinstitut, University of Bayreuth.

10.1021/jp045605m CCC: $30.25
Published on Web 02/22/2005

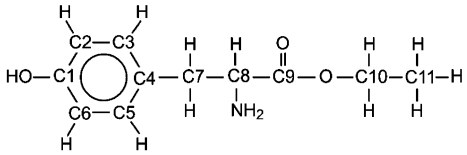

Figure 1. Schematic representation of the l-tyrosine-ethylester (TEE) molecule according to nomenclature used in ref 13.

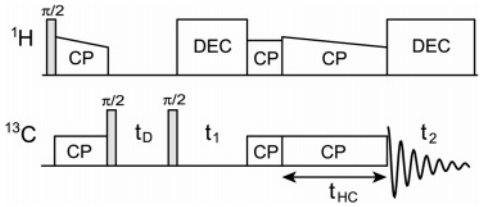

Figure 2. Pulse scheme for one- or two-dimensional CHC polarization transfer under MAS conditions. After an initial CP transfer and a *z*-filter to remove any residual ^{1}H magnetization, ^{13}C chemical shifts are recorded along the t_1 evolution time. After a short CP back-transfer step (175 μs), H−C dipolar interactions are monitored for a variable mixing time t_{HC} and finally recorded in t_2.

^{13}C chemical shifts are recorded along the t_1 evolution time. Next, a short CP step ensures that only ^{1}H magnetization of $C(H)_x$ groups is created. Establishing (^{1}H,^{13}C) CP for a variable mixing time t_{HC} allows for transfer to nearby ^{13}C spins that is read out along t_2. The second CP contact was established for 175 μs, while the final CP mixing unit was set to 1.5 ms (see also refs 21,22). Note that the pulse scheme described[21] can be modified to include a homonuclear (^{1}H,^{1}H) decoupling unit during (^{1}H,^{13}C) CP.

Rotational resonance in the tilted rotating frame (R^2TR) [23−25] was used to probe the C11−C2 distance in U[^{13}C]-TEE_{dil}. Two-dimensional constant-time experiments were performed for mixing times of 3.1, 5.2, and 7.5 ms at a MAS frequency of 10790 Hz. The R^2TR condition for the chemical shift difference of 10280 Hz was established by an additional low-power pulse of 1.64 kHz, framed by short (35-μs) ramp-in and ramp-out pulses.[24] Another set of R^2TR spectra for shorter mixing times of 0.8 and 2.6 ms was recorded for the spin pair C4−C7, which served to calibrate parameters for the quantum mechanical simulation of the C11−C2 cross-peak buildup (see below).

Lee−Goldburg[26] cross polarization[20] (LG-CP) transfers were set up using adamantane following well-established procedures.[27] LG-CP buildup measurements were performed at a MAS frequency of 10900 kHz in order to avoid rotational resonance[28] conditions. The applied field strengths during the LG-CP was $\omega_{1H,eff}/2\pi \approx 48$ kHz, and $\omega_{13C}/2\pi \approx 37$ kHz.

2.3. Quantum Mechanical Calculations. Quantum mechanical calculations using the C++ software library GAMMA[29] were carried out to simulate the cross-peak buildup for the C11−C2 spin pair in R^2TR experiments[25] and for the analysis of the LG-CP experiments. As noted elsewhere,[7] a quantum mechanical analysis does not adequately describe the details of proton−proton interactions in the solid state. In the R^2TR experiments, the relevant spin system comprises the nuclear spins of interest (C11, C2), as well as the directly bonded ^{13}C nuclei (C10, C3, C1) and all ^{1}H spins directly bonded to the aforementioned five carbon atoms.[25] Methylene and methyl protons were taken as single spins assuming a one-bond CH distance of 1.09 Å. Test calculations in smaller spin systems (data not shown) reveal that proton−proton interactions within the C10 methylene group, that were not taken into account due to reasons of computational time, are of minor influence.

Simulations under LG-CP conditions were conducted using rf fields as given by the experiment. In the case of nonuniaxial motion, the apparent CH coupling under Lee−Goldburg irradiation depends on the motionally scaled dipolar coupling, and the details of the transfer profile are affected by a nonzero asymmetry parameter.[30] However, the polarization transfer dynamics are also influenced by multiple-spin effects and experimental aspects such as rf inhomogeneity and pulse imperfections. Hence, only an overall phenomenological scaling parameter S of the dipolar coupling $D_{eff} = S \times D_{CH}$ with $D_{CH} = \mu_0\gamma_{13C}\gamma_{1H}\hbar/4\pi r_{CH}^3$ (see also ref 31) was used to reproduce the experimentally detected buildup characteristics. The 2-, 3-, and 4-spin systems were considered to simulate the polarization transfer dynamics of CH, CH_2, and CH_3 groups, respectively. While one-bond CH distances were set to 1.09 Å, HH distances of 1.75 and 1.63 Å were assumed for CH_2 and CH_3 groups, respectively. For the simulation of the methyl group (C11), an additional CH scaling factor of $S_{CH} = 1/3$ was introduced.[32]

2.4. Structure Calculation. Model structures were calculated using CNS.[33] Internuclear distances obtained from CHHC and R^2TR experiments were incorporated in the structure calculation by square-well distance restraints.[7] Ambiguous ^{1}H−^{1}H or ^{1}H−^{13}C restraints from methylene and methyl protons were accounted for by a sum averaging over all possible contacts. An elongated conformer of TEE was generated starting from the tyrosine amino acid parameter set in the PROTEIN-ALLHDG parameter files supplied with CNS version 1.1.[34] In the generated starting structure, the distance between C11 and C1 amounts to 8.3 Å. A set of 50 conformers was calculated using a simulated annealing protocol consisting of three stages: (1) high-temperature annealing in torsion angle space, in 2000 time steps of 0.002 ps at 30000 K; (2) slow-cool annealing stage in torsion angle space, in 6000 steps of 0.002 ps, and temperature reduction from 30000 K to zero in steps of 250 K; (3) final conjugate gradient minimization in 20 cycles of 200 steps each. Distance restraints were invoked by force constants of 150 kcal mol^{-1} Å^{-2} during all three annealing stages. The resulting structures were sorted by total energy. Sets of 15 out of 50 structures were chosen to represent the molecular structure of TEE.

Detailed restraint classifications are given as Supporting Information. Compared to our earlier model study on a tripeptide[7] where results of one 2D correlation experiment were used in a simplified, dual constraint classification, knowledge of the CHHC buildup characteristics here allows for a further refinement of the relationship between CHHC transfer efficiency and proton−proton distance. Three intervals were established corresponding to strong, medium, and weak transfer efficiencies. To account for missing cross-peaks, an additional segment was introduced. For cross validation, the final set of structures was used to compute transfer CHHC profiles using the relaxation model introduced in ref 7. As shown in the Supporting Information, these transfer curves compare favorably to the experimental results.

3. Results and Discussion

3.1. Low-Temperature Analysis of TEE. Earlier variable-temperature ^{13}C MAS NMR experiments[13] indicate that TEE exhibits phenyl ring π-flips with an activation energy of $E_a = 50 \pm 12$ kJ mol^{-1} at a sufficiently small flip rate at temperatures $T < 270$ K. Thus, CHHC spectra were obtained at 261 K for a ^{1}H−^{1}H mixing time of 250 μs. These are depicted in Figure 3,

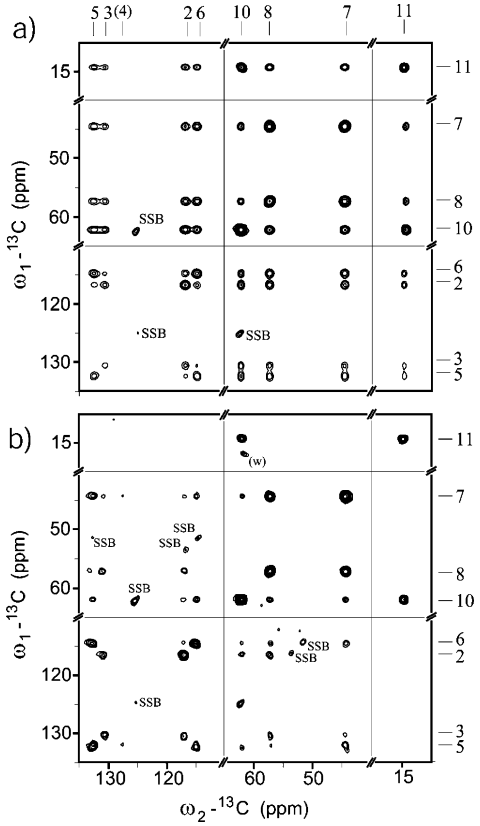

Figure 3. CHHC spectrum for a ^{1}H−^{1}H mixing time of 250 μs of *U*-[^{13}C]TEE (a) and *U*-[^{13}C]TEE$_{dil}$ (b) obtained on a 600 MHz WB instrument. Spinning sidebands (SSB) are indicated.

comparing results obtained on *U*-[^{13}C]TEE (a) and on *U*-[^{13}C]-TEE$_{dil}$ (b). As expected for the basic CHHC concept, resonances of the nonprotonated C1, C4, and C9 carbon atoms are strongly suppressed in all CHHC correlation data discussed in the following. On the other hand, a variety of (^{13}C,^{13}C) cross-peaks mediated by proton−proton interactions can be readily detected. While in Figure 3a correlations are seen among almost all ^{13}C resonances, a distinct set of (^{13}C,^{13}C) correlations is visible in Figure 3b. Correspondingly, the data in Figure 3a could be further used to monitor intermolecular interactions;[35] in the following, results obtained on *U*-[^{13}C]TEE$_{dil}$ will serve to study the structure and dynamic properties of the molecular moiety in solid TEE. As discussed in further detail elsewhere,[7] structural information can be obtained from CHHC 2D data if cross-peak intensities are evaluated in the initial rate regime and by analyzing transfer data obtained from several mixing times. For this reason, a series of CHHC experiments with mixing times of 75−500 μs were conducted (see Material and Methods section). As an example, Figure 4 contains data involving C8-to-ring correlations highlighting the qualitative difference between correlations involving C3 and C5: cross-peaks reflecting C8−C3 interactions build up faster than those originating from C8−C5 interactions, suggesting that the H_{C8}−H_{C3} distance must be significantly shorter than the H_{C8}−H_{C5} distance. In contrast to broadband (^{13}C,^{13}C) correlation experiments, indirect detection of (^{1}H,^{1}H) interactions hence allows for the spectral identification of each ring carbon.

As discussed in further detail in ref 13, total through-space (^{13}C,^{13}C) correlation spectroscopy[36] does not provide a definitive answer as to whether TEE adopts an elongated or "scorpion-like" structure in the polycrystalline state. For this aspect, ^{1}H−^{1}H contacts mediating (^{13}C,^{13}C) correlations of C10 and C11 with ring carbons are of particular interest. As can be seen from Figure 3b, patterns correlating C10 with nuclei in the ring (C2,3,5,6) can be readily identified for short mixing times, consistent with proton−proton contacts over a length scale of 3 Å. Since these data are obtained from the diluted sample *U*-[^{13}C]TEE$_{dil}$, these interactions must reflect intramolecular interactions and thus provide information about molecular conformation.

A series of buildup curves for one-bond and ethylester−phenyl-ring cross-peak intensities is displayed in Figure 5. The data were obtained by dividing the sum of the cross-peak volumes for each pair of spins by the sum of the corresponding diagonal peak volumes as a function of mixing time. Directly bonded ^{13}C nuclei show the strongest ^{1}H−^{1}H polarization transfer (such as C7−C8), and buildup curves for these nuclei agree well with the CHHC transfer characteristics studied in other model compounds under comparable experimental conditions.[7] Interestingly, the buildup of the one-bond C10−C11 correlation is slightly slower than for all other one-bond interactions considered in (a). This could be consistent with a reduction in (^{1}H,^{1}H) polarization transfer efficiency due to the methyl group rotation. Notably, earlier rotational-resonance (R^2) ^{13}C experiments concerning the C10−C11 pair of spins in *U*-[^{13}C]TEE also indicate a seemingly reduced effective C10−C11 dipolar coupling constant.[37] From Figure 5b, a variety of C10−phenyl-ring correlations can be observed at $t_{HH} \geq 150$ μs. On the other hand, C11−phenyl-ring correlations are in general weaker than those involving C10 and start to appear only for a mixing time of 500 μs. As discussed in further detail in ref 7, cross-peak intensities detected for such long mixing times may reflect relay transfer involving more than two proton spins, making a direct structural analysis difficult. We also observe notable differences regarding (^{1}H,^{1}H) correlations among phenyl-ring carbon atoms. Nearest-neighbor interactions, i.e., C2−C3 and C5−C6, are visible for very short proton−proton mixing times (Figure 3b). C3−C5 and C2−C6 correlations appear for $t_{HH} \geq 150$ μs. C3−C6 and C5−C2 interactions are not detected even for a mixing time of 500 μs. The latter findings fully agree with the spectral assignments used in Figures 3 and 4 that would require polarization transfer across the ring diagonal (i.e., 6 Å, Figure 1), which is strongly attenuated for the considered mixing times.

An independent means of probing molecular structure is brought about by measuring (^{13}C,^{1}H) correlations in two spectral dimensions. For this purpose, the N/CHHC polarization transfer concept[18] can be modified by removing the proton−proton mixing block and using the final CP polarization block as a variable (^{1}H,^{13}C) transfer unit.[21] The corresponding NHC transfer scheme has recently been used for measuring intermolecular transfer in molecular mixtures.[22] Figure 6 shows that a mixing time t_{HC} of 1.5 ms delivers a multitude of through-space interactions in a CHC experiment applied to *U*-[^{13}C]TEE$_{dil}$. In addition to CHHC correlations involving two protonated carbon atoms, correlations relating to C1, C4, and C9 resonances can now be observed. For the mixing time used, correlations of C1 with other nuclei are seen only within the phenyl ring, with more intense cross-peaks to C2 and C6 than for C3 and C5. On the other hand, a variety of three-bond correlations such as (C11,C9), (C10,C8), and (C4,C8) are detected. A cross-peak between the resonances of nonprotonated carbons C4 and C9, also within a range of three bonds, is absent, as expected. Cross-peaks relating the ester tail to the ring reveal qualitative agreement with the structural constraints derived from the CHHC correlations. As shown in ref 22, CHC-type transfer is, however, also influenced by the MAS rate. For this reason, a

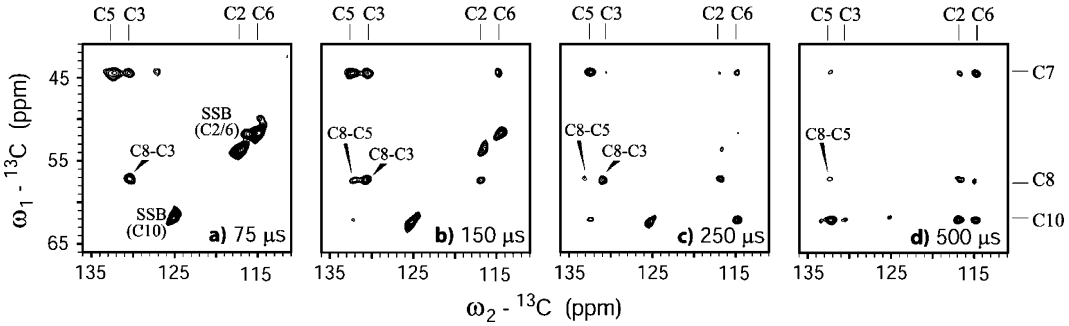

Figure 4. Series of CHHC spectra with different mixing times, showing a spectral region with cross-peaks of carbon resonances in the aromatic ring.

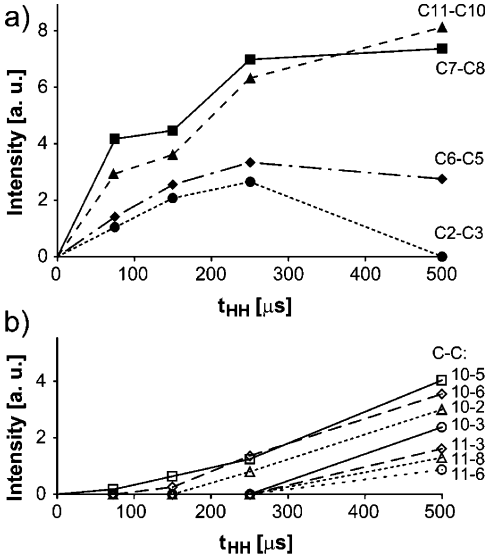

Figure 5. Intensity buildup of selected CHHC cross-peaks for one-bond (a) and ester-tail−ring (b) ^{1}H−^{1}H interactions.

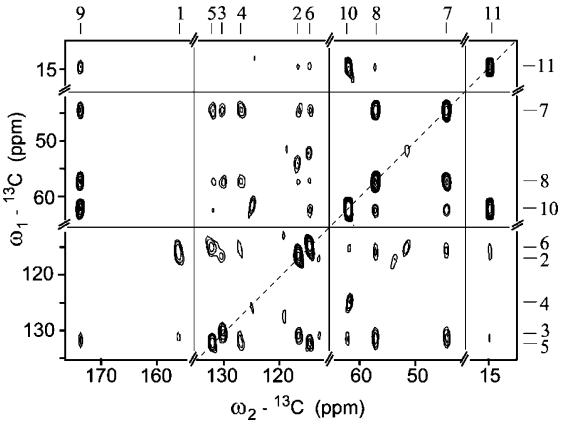

Figure 6. CHC spectrum obtained on *U*-[^{13}C]TEE$_{dil}$ at 261 K. t_{HC} was set to 1.5 ms.

direct structural interpretation of the CHC correlation was not attempted here.

To further elucidate the structural topology involving the (C11,C2) pair of spins, we conducted 2D constant-time[25] R^2-TR[23] experiments using mixing times of 3.1, 5.2, and 7.5 ms. In Figure 7 (mixing time 5.2 ms), cross-peaks can be readily identified without spectral overlap with the resonances of the pair of spins (^{13}C11, ^{13}C2). The measured cross-peak buildup was further compared to a quantum mechanical calculation, with the C11−C2 bond distance amounting to 4.9 Å (Figure 7, vide infra). As discussed in more detail elsewhere,[25] the accuracy of the distance determination, however, strongly depends on

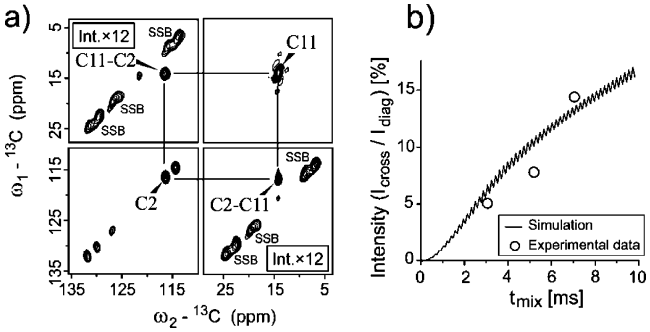

Figure 7. (a) Close-up of the spectral region of the C11−C2 diagonal and cross-peaks for a R^{2}TR experiment with a 5.2-ms mixing time. Cross-peaks are separated by 510 Hz relative to the spinning sidebands (SSB). For the sake of clarity, intensities in the cross-peak region are scaled up by a factor of 12. (b) Comparison of measured cross-peak intensities for three different mixing times (open circles) with simulated cross-peak buildup (solid line).

experimental conditions, in particular on proton decoupling field strength during (^{13}C,^{13}C) mixing.

The distance restraints obtained from the analysis of our CHHC and R^{2}TR experiments were finally utilized in a standard 3D structure calculation within CNS. As shown in Figure 8b, the use of CHHC distance restraints leads to a reduction of the available conformational space of TEE (Figure 8a) and firmly establishes the scorpion-like fold of the molecule in the crystalline state. One R^{2}TR distance restraint (Figure 8c) alone is, on the other hand, insufficient to adequately describe the molecular structure of TEE at low temperatures, but it helps to further refine the CHHC-based structural model of TEE (Figure 8d).

3.2. Solid-State NMR Analysis at Higher Temperature. The phenyl ring in solid TEE undergoes π-flips at higher temperatures; as a result of this, chemical-exchange broadening prevents the spectral separation of the ^{13}C3/5 and ^{13}C2/6 resonances[13] at temperatures $T > 318$ K. To investigate the influence of molecular dynamics upon (^{1}H,^{1}H) transfer, a CHHC spectrum of *U*-[^{13}C]TEE$_{dil}$ was recorded with a mixing time of 250 μs at 318 K (Figure 9). Similar to Figure 3b, correlations of the phenyl-ring carbon resonances to C7, C8, and C10 resonances can be observed, albeit with an overall lower signal-to-noise ratio. Again, C11 shows cross-peaks only with C10 for the given signal-to-noise ratio. For a more detailed analysis, we compare in Figure 10 the normalized CHHC cross-peak intensities at low (261 K) and high (318 K) temperatures. Although the overall signal intensity is decreased, the general transfer behavior is similar, suggesting that the overall structure (defined by nearest-neighbor proton−proton interactions) is preserved at higher temperature. Notably, this conclusion would also be consistent with a ring flip that, as predicted in ref 13,

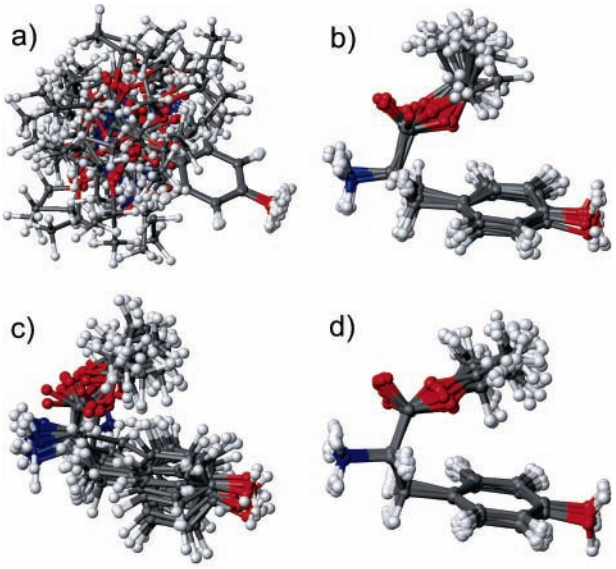

Figure 8. (a) Complete ensemble of 50 structures calculated without additional experimental distance restraints. Structures do not differ significantly in total energy. (b) Ensemble of 15 out of 50 calculated structures representing TEE as seen by CHHC spectroscopy at low temperatures. (c) Ensembles with 20 out of 50 structures for TEE calculated using one C11−C2 distance restraint from R^2TR alone. (d) Structure calculation using a combination of CHHC restraints at 261 K and one R^2TR distance restraint.

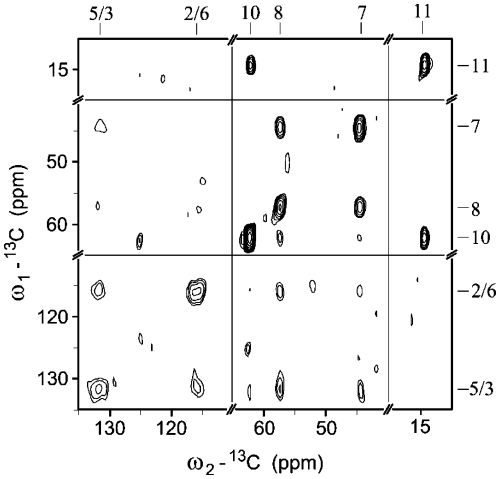

Figure 9. CHHC spectrum for a ^{1}H−^{1}H mixing time of 250 μs at 318 K. Resonance lines from exchanging ring sites overlap.

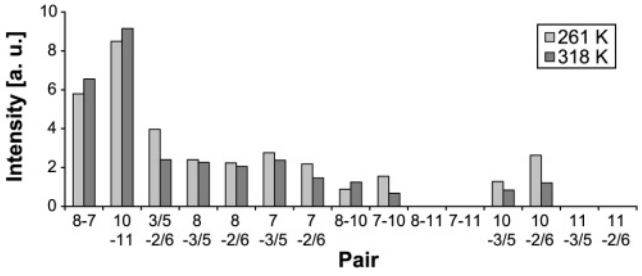

Figure 10. CHHC cross-peak amplitudes for the different TEE spin pairs for experiments conducted at two different temperatures. Intensities X/Y given at low temperatures reflect the sum of signal amplitudes measured for resonances X and Y. All cross-peak intensities were normalized to the total intensity of the 2D spectrum.

would occur on a time scale significantly longer than the inverse of the polarization transfer rate for proton−proton distances in the order of 3.5 Å.

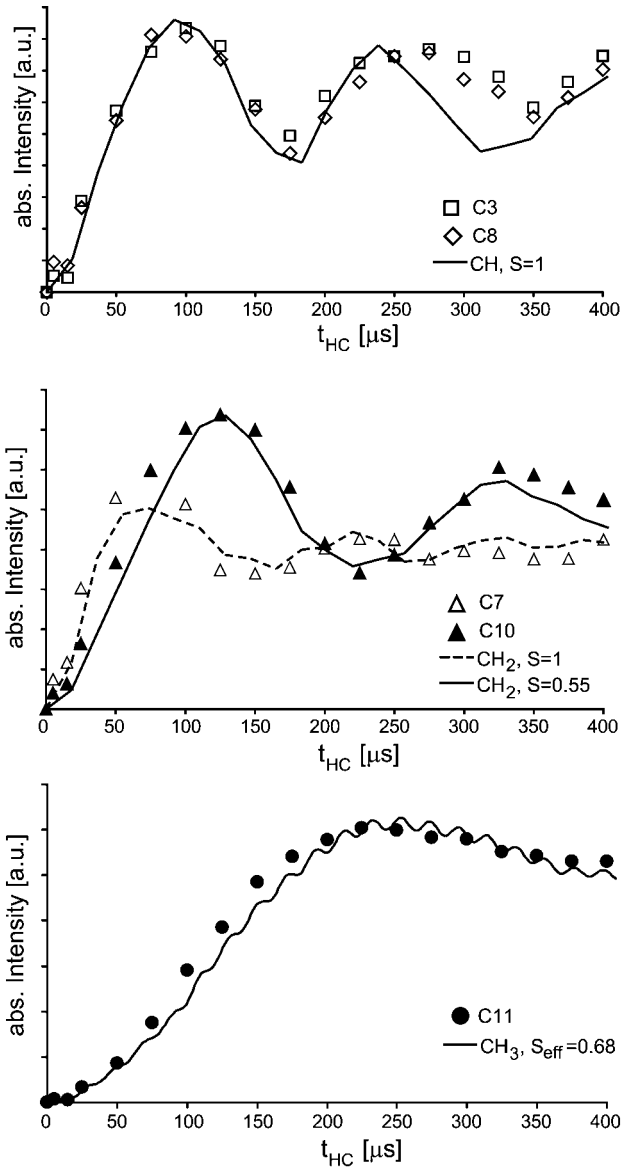

Figure 11. LG-CP buildups for C8 (open diamond) and C3 (open square) (a), C7 (open triangle) and C10 (solid triangle) (b), and C11 (c). Numerical simulations were conducted for systems of 2−4 spins and are included as (solid or dashed) lines.

3.3. Molecular Dynamics As Seen by LG-CP. So far, the structural characterization of TEE was based on the detection of (^{1}H,^{1}H) contacts and (^{13}C,^{13}C) distance constraints that report on the 3D molecular arrangement. The underlying dipolar coupling interactions depend on the through-space distance but can be modulated by molecular motion. As an independent means to study molecular dynamics, solid-state NMR experiments that probe one-bond (^{13}C,^{13}C) and (^{1}H,^{13}C) dipolar interactions at variable temperatures may be employed. Since one-bond distances are well-known for both interactions, measurements of the corresponding effective dipolar coupling constants hence can reveal the effects of dynamic averaging. To suppress unwanted signal modulations due to (^{1}H,^{1}H) interactions during HC transfer, a variety of homonuclear decoupling schemes have been suggested.[38,39] We rely in the following on the measurement of the cross polarization ^{13}C buildup under Lee−Goldburg[26,30,39] conditions. In Figure 11, results are shown for C8, C5 (CH, a), C7, C10 (CH_2, b), and C11 (CH_3, c) resonances as a function of the LG-CP buildup time. As discussed in section 2, numerical simulations were

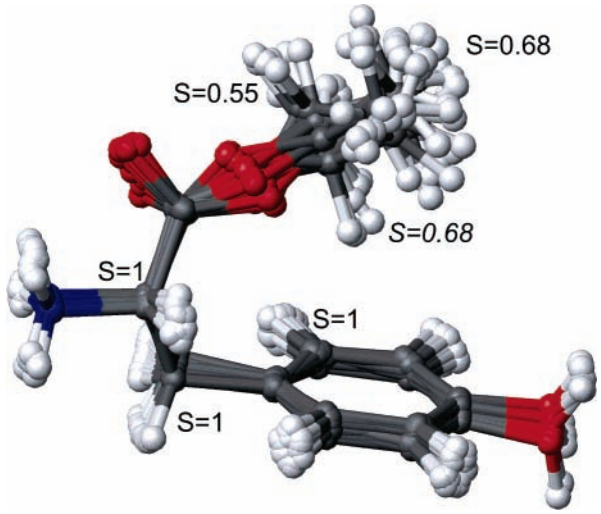

Figure 12. Molecular model of polycrystalline TEE derived from the measurement of CHHC distance parameters and one (^{13}C,^{13}C) distance restraint. Order parameters have been obtained from Figure 11 and (given in italics) results discussed in ref 13.

conducted for systems of 2−4 spins assuming rf fields and resonance offsets as employed in the experiments. As visible from Figure 11a, the one-bond CH spin dynamics are well reproduced, assuming a dipolar order parameter $S = 1$ for C8 and C5. The latter observation is in accordance with a general notion that π-ring flips in TEE at lower temperatures occur on a time scale slower than the CH dipolar interaction. At higher temperatures, the CH coupling of ring carbon atoms can be further modulated[12] and a nonuniaxial motion must be considered.[30] On the contrary, the CP buildup characteristics of the ^{13}C10 resonance can only be reproduced using scaling factors $S_{CH} = S_{HH} = 0.55$. A similar scaling factor ($S_{eff} = 0.68$) is found for the C11 spin if an overall methyl group rotation is taken into account. These results hence indicate an increase in molecular mobility for the ester tail, in agreement with results of broadband (^{13}C,^{13}C) 1Q correlation spectroscopy,[13] and lead to a molecular order parameter for the ^{13}C10−^{13}C11 dipolar coupling tensor of 0.68. In agreement with ref 13, the order parameters observed for C10 and C11 are not affected by an increase in temperature from 261 to 318 K, suggesting that the 3D structure derived at lower temperatures is largely preserved at higher temperatures and can be described by the order parameters shown in Figure 12.

As discussed in ref 13,[3] broadband (^{13}C,^{13}C) 1Q correlation spectroscopy already leads the way to models of the dynamic disorder affecting the ester tail of solid TEE. These NMR data are, for example, consistent with rapid nutation in a 25−30° cone around the C10−C11 bond axis.[13] As discussed above, molecular mobility also affects the LG-CP buildup characteristics. Assuming an axially symmetric motion, the corresponding order parameters can be related to the root-mean-square (rms) angular fluctuations[40] via the following equation:

$$S = \frac{3\cos^2\theta - 1}{2} \qquad (1)$$

For the ^{13}C−^{1}H spin pairs, one finds rms angular fluctuations of 33° (C10) and 28° (C11). Compared to the structural ensemble calculated from CHHC data, these parameters are well within the range of structural accuracy of the ester tail. Molecular mobility should also affect results of (^{13}C,^{13}C) distance measurements as discussed in section 3.1 for R^{2}TR mixing, or as reported for rotational resonance (R^2) experiments conducted on a selectively [^{13}C10,^{13}C1]-labeled TEE sample.[41] The proposed cone motion would lead to fluctuations of the (^{13}C,^{13}C) ester−ring distance of 0.5−0.75 Å, which is close to the error margins reported for R^2 and R^{2}TR experiments.[25,41]

4. Conclusions

In many biomolecular systems, information about both 3D structure and residual dynamics is of paramount importance for understanding biochemical functions such as protein folding, ligand binding, and protein−protein interactions. As is demonstrated here for TEE, constraints defining the 3D structure of a molecule are readily available using CHHC correlation experiments that indirectly probe nearest-neighbor (^{1}H,^{1}H) interactions in high spectral resolution. These experiments confirm, in agreement with the findings of single-crystal X-ray diffraction, that the TEE molecule in the solid crystalline state adopts a scorpion-like structure. Assuming conservative (^{1}H,^{1}H) distance constraints, the accuracy of the derived structure can be further improved by R^{2}TR 2D correlation experiments. While the location of the C10 atom relative to the phenyl ring is rather well-defined, C11−phenyl ring (^{1}H,^{1}H) contacts are weak, leading to disorder in the resulting solid-state NMR model of TEE. An analysis of ^{13}C−^{13}C and ^{13}C−^{1}H one-bond interactions suggests that structural disorder is induced by molecular dynamics of the ester tail that is largely constant in the considered temperature range. Angular fluctuations deduced from the molecular order parameters are in qualitative agreement with the accuracy of 3D structure.

As demonstrated here for TEE, the detection of through-space (^{1}H,^{1}H) and (^{13}C,^{13}C) interactions and one-bond dipolar couplings can provide an efficient means to detect molecular structure and dynamic disorder at atomic resolution. In particular, the combined application of both NMR techniques permits a clear distinction of structural or dynamic disorder in the solid state. Such information is, for example, relevant in the context of studying membrane penetration and insertion in a variety of biomolecules or may help characterizing ligand−receptor interactions in a noncrystalline environment.

Acknowledgment. This work was funded in part by the Deutsche Forschungsgemeinschaft, Aventis/ Paris, and the MPG.

Supporting Information Available: Information on the distance restraints used within CNS and the corresponding CHHC transfer dynamics expected from theory is given. Furthermore, transfer profiles as expected from the final 3D TEE structures are compared to experimental data points. This material is available free of charge via the Internet at http://pubs.acs.org.

References and Notes

(1) Brown, S. P.; Spiess, H. W. *Chem. Rev.* **2001**, *101*, 4125−4155; Tycko, R. *Curr. Opin. Chem. Biol.* **2000**, *4*, 500−506; Luca, S.; Heise, H.; Baldus, M. *Acc. Chem. Res.* **2003**, *36*, 858−865.

(2) Griffin, R. G. *Nat. Struct. Biol.* **1998**, *5*, 508−512.

(3) Opella, S. J.; Marassi, F. M. *Chem. Rev.* **2004**, *104*, 3587−3606.

(4) Dusold, S.; Sebald, A. *Annu. Rep. NMR Spectrosc.* **2000**, *41*, 185−264; Levitt, M. H. In *Encyclopedia of Nuclear Magnetic Resonance: Supplementary Volume*; Grant, D. M., Harris, R. K., Eds.; Wiley: Chichester, 2002; pp 165−196.

(5) Cross, T. A.; Opella, S. J. *Curr. Opin. Struct. Biol.* **1994**, *4*, 574−581; Petkova, A. T.; Ishii, Y.; Balbach, J. J.; Antzutkin, O. N.; Leapman, R. D.; Delaglio, F.; Tycko, R. *Proc. Natl. Acad. Sci.* **2002**, *99*, 16742−16747; Jaroniec, C. P.; MacPhee, C. E.; Astrof, N. S.; Dobson, C. M.; Griffin, R. G. *Proc. Natl. Acad. Sci.* **2002**, *99*, 16748−16753; Jaroniec, C. P.; MacPhee, C. E.; Bajaj, V. S.; McMahon, M. T.; Dobson, C. M.; Griffin, R. G. *Proc. Natl. Acad. Sci. U.S.A.* **2004**, *101*, 711−716; Castellani, F.; van Rossum, B.; Diehl, A.; Schubert, M.; Rehbein, K.; Oschkinat, H. *Nature*

2002, *420*, 98−102; Rienstra, C. M.; Tucker-Kellogg, L.; Jaroniec, C. P.; Hohwy, M.; Reif, B.; McMahon, M. T.; Tidor, B.; Lozano-Perez, T.; Griffin, R. G. *Proc. Natl. Acad. Sci. U.S.A.* **2002**, *99*, 10260−10265.

(6) Nomura, K.; Takegoshi, K.; Terao, T.; Uchida, K.; Kainosho, M. *J. Am. Chem. Soc.* **1999**, *121*, 4064−4065; Lange, A.; Becker, S.; Seidel, K.; Pongs, O.; Baldus, M. *Angew. Chem., Int. Ed. Engl.*, in press.

(7) Lange, A.; Seidel, K.; Verdier, L.; Luca, S.; Baldus, M. *J. Am. Chem. Soc.* **2003**, *125*, 12640−12648.

(8) Palmer, A. G.; Williams, J.; McDermott, A. *J. Phys. Chem.* **1996**, *100*, 13293−13310.

(9) Seelig, J.; Gally, H. U. *Biochemistry* **1976**, *15*, 5199−5204.

(10) Schmidt-Rohr, K.; Spiess, H. W. *Multidimensional Solid-state NMR and Polymers*; Academic Press: London/San Diego, 1994.

(11) Torchia, D. A. *Annu. Rev. Biophys. Bioeng.* **1984**, *13*, 125−144; Keniry, M. A.; Gutowsky, H. S.; Oldfield, E. *Nature* **1984**, *307*, 383−386; Lewis, B. A.; Harbison, G. S.; Herzfeld, J.; Griffin, R. G. *Biochemistry* **1985**, *24*, 4671−4679.

(12) Frey, M. H.; Diverdi, J. A.; Opella, S. J. *J. Am. Chem. Soc.* **1985**, *107*, 7311−7315.

(13) Helluy, X.; Sebald, A. *J. Phys. Chem. B* **2003**, *107*, 3290−3296.

(14) Andrew, E. R.; Bradbury, A.; Eades, R. G. *Nature* **1958**, *182*, 1659.

(15) Luca, S.; White, J. F.; Sohal, A. K.; Filippov, D. V.; van Boom, J. H.; Grisshammer, R.; Baldus, M. *Proc. Natl. Acad. Sci. U.S.A.* **2003**, *100*, 10706−10711.

(16) Pieret, A. F.; Durant, F.; Griffe, M.; Germain, G. *Acta Crystallogr., Sect. B—Struct. Crystallogr. Cryst. Chem.* **1970**, *B 26*, 2117−2119.

(17) Bennett, A. E.; Rienstra, C. M.; Auger, M.; Lakshmi, K. V.; Griffin, R. G. *J. Chem. Phys.* **1995**, *103*, 6951−6958.

(18) Lange, A.; Luca, S.; Baldus, M. *J. Am. Chem. Soc.* **2002**, *124*, 9704−9705.

(19) Heise, H.; Seidel, K.; Etzkorn, M.; Becker, S.; Baldus, M. *J. Magn. Reson.* **2005**, *173*, 64−74.

(20) Hartmann, S. R.; Hahn, E. L. *Phys. Rev.* **1962**, *128*, 2042−2053; Pines, A.; Gibby, M. G.; Waugh, J. S. *J. Chem. Phys.* **1973**, *59*, 569−590.

(21) Lange, A. Diploma thesis, University Göttingen, 2002.

(22) Etzkorn, M.; Böckmann, A.; Lange, A.; Baldus, M. *J. Am. Chem. Soc.* **2004**, *126*, 14746−14751.

(23) Takegoshi, K.; Nomura, K.; Terao, T. *Chem. Phys. Lett.* **1995**, *232*, 424−428.

(24) Costa, P. R.; Sun, B. Q.; Griffin, R. G. *J. Am. Chem. Soc.* **1997**, *119*, 10821−10830.

(25) Sonnenberg, L.; Luca, S.; Baldus, M. *J. Magn. Reson.* **2004**, *166*, 100−110.

(26) Lee, M.; Goldburg, W. I. *Phys. Rev.* **1965**, *140*, 1261−1271.

(27) Bielecki, A.; Kolbert, A. C.; Levitt, M. H. *Chem. Phys. Lett.* **1989**, *155*, 341−346.

(28) Raleigh, D. P.; Levitt, M. H.; Griffin, R. G. *Chem. Phys. Lett.* **1988**, *146*, 71−76.

(29) Smith, S. A.; Levante, T. O.; Meier, B. H.; Ernst, R. R. *J. Magn. Reson. Ser. A* **1994**, *106*, 75−105; Metz, G.; Wu, X. L.; Smith, S. O. *J. Magn. Reson., Ser. A* **1994**, *110*, 219−227.

(30) Hong, M.; Yao, X. L.; Jakes, K.; Huster, D. *J. Phys. Chem. B* **2002**, *106*, 7355−7364.

(31) Baldus, M. *Prog. Nucl. Magn. Reson. Spectrosc.* **2002**, *41*, 1−47.

(32) Munowitz, M.; Aue, W. P.; Griffin, R. G. *J. Chem. Phys.* **1982**, *77*, 1686−1689.

(33) Brunger, A. T.; Adams, P. D.; Clore, G. M.; DeLano, W. L.; Gros, P.; Grosse-Kunstleve, R. W.; Jiang, J. S.; Kuszewski, J.; Nilges, M.; Pannu, N. S.; Read, R. J.; Rice, L. M.; Simonson, T.; Warren, G. L. *Acta Crystallogr., Sect. D—Biol. Crystallogr.* **1998**, *54*, 905−921.

(34) Nilges, M. *Curr. Opin. Struct. Biol.* **1996**, *6*, 617−623.

(35) Tycko, R.; Ishii, Y. *J. Am. Chem. Soc.* **2003**, *125*, 6606−6607; de Boer, I.; Matysik, J.; Amakawa, M.; Yagai, S.; Tamiaki, H.; Holzwarth, A. R.; de Groot, H. J. M. *J. Am. Chem. Soc.* **2003**, *125*, 13374−13375.

(36) Baldus, M.; Tomaselli, M.; Meier, B. H.; Ernst, R. R. *Chem. Phys. Lett.* **1994**, *230*, 329−336; Baldus, M.; Meier, B. H. *J. Magn. Reson.* **1997**, *128*, 172−193.

(37) Dusold, S.; Sebald, A. *J. Magn. Reson.* **2000**, *145*, 340−356.

(38) Caravatti, P.; Braunschweiler, L.; Ernst, R. R. *Chem. Phys. Lett.* **1983**, *100*, 305−310; Gross, J. D.; Warschawski, D. E.; Griffin, R. G. *J. Am. Chem. Soc.* **1997**, *119*, 796−802.

(39) van Rossum, B. J.; de Groot, C. P.; Ladizhansky, V.; Vega, S.; de Groot, H. J. M. *J. Am. Chem. Soc.* **2000**, *122*, 3465−3472.

(40) Lipari, G.; Szabo, A. *J. Am. Chem. Soc.* **1982**, *104*, 4546−4559.

(41) Raleigh, D. P.; Creuzet, F.; Gupta, S. K. D.; Levitt, M. H.; Griffin, R. G. *J. Am. Chem. Soc.* **1989**, *111*, 4502−4503.